Identification and Characterization of Genetic Variation in the Folylpolyglutamate Synthase Gene

Tarek A. Leil,[1] Chiaki Endo,[2] Araba A. Adjei,[3] Grace K. Dy,[4] Oreste E. Salavaggione,[5] Joel R. Reid,[1] Matthew M. Ames,[1] and Alex A. Adjei[5]

[1]Department of Oncology, Mayo Clinic, Rochester, Minnesota; [2]Department of Thoracic Surgery, Institute of Development, Aging, and Cancer, Tohoku University, Sendai, Japan; Departments of [3]Pharmacology and [4]Medicine, Roswell Park Cancer Institute, Buffalo, New York; and [5]Department of Pathology, Washington University School of Medicine, St. Louis, Missouri

Abstract

Folylpolyglutamate synthase (FPGS) catalyzes the polyglutamation of folic acid, methotrexate, and pemetrexed to produce highly active metabolites. To characterize genetic variation in the FPGS gene, *FPGS,* have resequenced the gene in four different ethnic populations. Thirty-four single nucleotide polymorphisms were identified including five nonsynonymous coding single nucleotide polymorphisms that altered the FPGS protein sequence: F13L and V22I polymorphisms in the mitochondrial isoform of FPGS, and R466/424C, A489/447V, and S499/457F polymorphisms, which exist in both the mitochondrial and cytosolic isoforms. When expressed in AuxB1 cells, the A447V cytosolic variant was functionally similar to the wild-type cytosolic (WT Cyt) allozyme, whereas the R424C and S457F cytosolic variants were reduced by ~2-fold in protein expression compared with WT Cyt ($P < 0.01$). The intrinsic clearance of glutamate was reduced by 12.3-fold (R424C, $P < 0.01$) and 6.2-fold (S457F, $P < 0.01$), whereas the intrinsic clearance of methotrexate was reduced by 4.2-fold (R424C, $P < 0.05$) and 5.4-fold (S457F, $P < 0.05$) in these two cytosolic variants when compared with the WT Cyt isoform. Additionally, the *in vitro* enzyme velocity at saturating pemetrexed concentrations was reduced by 1.6-fold (R424C, $P < 0.05$) and 2.6-fold (S457F, $P < 0.01$) compared with WT Cyt. AuxB1 cells harboring these same cytosolic variant allozymes displayed significant increases in the EC_{50} for folic acid and in the IC_{50} values for both methotrexate and pemetrexed relative to the WT Cyt form of FPGS. These observations suggest that genetic variations in *FPGS* may alter the efficacy of antifolate therapy in cancer patients. [Cancer Res 2007;67(18):8772–82]

Introduction

Drugs that target the folate pathway such as methotrexate and pemetrexed are effective treatments for many hematologic malignancies and solid tumors (1, 2). Both drugs are structural analogues of folic acid, both inhibit multiple enzymes in the folate pathway, and both require polyglutamation by folylpolyglutamate synthase (FPGS) for activation (3, 4). FPGS catalyzes the addition of multiple glutamate molecules to compounds with the basic pteroylglutamate structure (5) such as tetrahydrofolate and many folate analogues. Polyglutamation of endogenous reduced folates is the cellular mechanism for retention and accumulation of these essential cofactors (6). In general, polyglutamyl derivatives of endogenous reduced folates have a much higher affinity for tetrahydrofolate cofactor–requiring enzymes than their unpolyglutamated forms (7). The same is true for most antifolates that are substrates for polyglutamation by FPGS. For example, although the K_i of methotrexate for dihydrofolate reductase is not altered significantly by polyglutamation, its affinity for thymidylate synthase, glycinamide ribonucleotide formyltransferase, and aminoimidazolecarboxamide ribonucleotide formyltransferase is dramatically increased upon polyglutamation (8). Similarly, pemetrexed also has dramatic increases in its affinity for thymidylate synthase, glycinamide ribonucleotide formyltransferase, and aminoimidazolecarboxamide ribonucleotide formyltransferase upon polyglutamation by FPGS (8). Polyglutamation of methotrexate and pemetrexed also leads to prolonged cellular retention. The activity of FPGS has been characterized as a possible predictive factor for antifolate treatment in some patients with cancer. In children with acute lymphoblastic leukemia, accumulation of methotrexate polyglutamates in lymphoblasts is correlated with improved 5-year survival (9) and increased short-term eradication of lymphoblasts by methotrexate treatment (10).

The human *FPGS* is 11.4 kb long, contains 15 exons and 14 introns, and is located on chromosome region 9q34.11 (11, 12). Alternative translational initiation of exon 1 produces two proteins, the predominant 537–amino acid residue cytosolic protein, and the mitochondrial protein with additional 42 amino acid residues at the NH_2 terminus (13). Both reduction of mRNA expression (14, 15) and spontaneous mutation of *FPGS* (16, 17) have been observed as mechanisms of resistance to antifolate treatment in cell culture.

Given the importance of polyglutamation on the clinical efficacy of antifolate drugs, it is important to examine the role of genetic variation in *FPGS* on the metabolism, pharmacokinetics, and pharmacodynamics of these drugs. Thus far, there have been no reports on the functional effects of polymorphisms in *FPGS* despite the fact that over 40 single nucleotide polymorphisms (SNP) are listed in the National Center for Biotechnology Information's dbSNP database. To address this issue, we have identified *FPGS* polymorphisms, most of which were previously unreported, by systematically resequencing the gene. We then focused on functionally characterizing the three cytosolic nonsynonymous coding SNPs (cSNP) observed. Our results indicate that two of the three cSNPs affected protein expression, *in vitro* substrate kinetics of the enzyme, and folate and antifolate efficacy in cells expressing the polymorphisms.

Materials and Methods

DNA samples. Two hundred and forty DNA samples from 60 African-American, 60 Caucasian-American, 60 Han Chinese-American, and

Note: Supplementary data for this article are available at Cancer Research Online (http://cancerres.aacrjournals.org/).

Requests for reprints: Alex A. Adjei, Department of Medicine, Roswell Park Cancer Institute, Elm and Carlton Streets, Buffalo, NY 14263. Phone: 716-845-4101; Fax: 716-845-3423; E-mail: alex.adjei@roswellpark.org.

doi:10.1158/0008-5472.CAN-07-0156

60 Mexican-American subjects (sample sets HD100CAU, HD100AA, HD100CHI, and HD100MEX) were obtained from the Coriell Cell Repository (Camden, NJ). All of these DNA samples had been anonymized by the National Institute of General Medical Sciences prior to being deposited, and all subjects had provided written consent for the use of their DNA for experimental purposes.

***FPGS* gene resequencing.** Gene resequencing was done as previously described (18). Specifically, all 15 exons, all exon-intron splice junctions, ~1.0 kb of the 5′-flanking region, all of the 5′-UTRs (untranslated region), and a portion of the 3′-UTR of *FPGS* were resequenced. PCR amplifications of areas to be resequenced were done for the 240 DNA samples. M13 "tags" were added to the 5′-ends of each primer to make it possible to use dye primer sequencing chemistry. The sequences of all the primers used for this resequencing project are listed in the supplementary data. Amplicons were sequenced on both strands in the Mayo Molecular Core Facility and the sequence was analyzed as described previously (18). To exclude PCR-induced artifacts, independent amplifications were done for those samples in which a SNP was observed only once, or for any sample with an ambiguous chromatogram. The *FPGS* consensus reference sequence used for comparison was NT_008470.16.

Expression of FPGS variants in AuxB1 cells. The wild-type cytosolic (WT Cyt) cDNA sequence for *FPGS* was initially cloned into the eukaryotic expression vector pCR3.1 (Invitrogen). The pCR3.1 WT Cyt *FPGS* expression construct was then used as the template for site-directed mutagenesis using circular PCR to create the variant constructs. The wild-type mitochondrial (WT Mit) FPGS was also generated as an additional expression construct. These constructs were then used as templates for PCR/TOPO TA cloning into pCRII TOPO (Invitrogen). The cDNAs were then excised from pCRII TOPO and cloned by restriction digestion (*Eco*RI and *Sal*I) into the modified pIRES-EGFP vector (Clontech) kindly donated by L. Karnitz (Mayo Clinic, Rochester, MN). The primers used for cloning and mutagenesis are listed in the supplementary data (Table S1). This vector (pSF-GFP) allows the fusion of a 3xFLAG epitope at the NH_2 terminus of the protein as well as expression of GFP on the same cistron as *FPGS* to allow for normalization of transfection efficiency. Sequences of all constructs were confirmed by sequencing both strands of the insert.

AuxB1 cells grown in complete α-minimal essential medium with nucleosides [α(+)MEM; Sigma] were transiently transfected with expression constructs for WT Cyt and WT Mit FPGS, the variant cytosolic allozymes, and the empty pSF-GFP vector using LipofectAMINE 2000 reagent (Invitrogen). Specifically, 20 μg of DNA was used to transfect 80% confluent AuxB1 cells in 100 mm plates as described in the vendor's instructions. Twenty-four to 48 h after transfection, the cells were harvested for *in vitro* or cell culture assays.

Detection and quantification of FPGS. AuxB1 cells transfected with the pSF-GFP FPGS allozyme expression constructs were harvested 24 h after transfection. Cells were homogenized in sonication buffer [0.1 mol/L Tris-HCl (pH 8.5), 10 mmol/L ATP, 25 mmol/L $MgCl_2$, 10 mmol/L DTT, 100 μg/mL leupeptin, 1 mmol/L phenylmethylsulfonyl fluoride, and 0.05% *n*-octylglucoside] and sonicated for 30 s at 30% power using a Branson sonifier 450. The homogenate was then centrifuged at 12,000 × *g* for 15 min. The supernatant was assayed for protein concentration using the DC Protein Assay (Bio-Rad) and then used either for ELISA or Western blot.

ELISA was done to quantify the levels of FPGS protein in AuxB1 cell extracts. Immulon 2HB 96-well ELISA plates (Thermo Electron Corporation) were coated overnight at 4°C with AuxB1 protein extracts diluted to 10 μg/mL in coating buffer (sodium bicarbonate buffer, pH 9.6). The 3xFLAG-BAP control protein (Sigma) was diluted in 10 μg/mL of bovine serum albumin and used to generate a standard curve. After coating, the wells of the ELISA plate were incubated with blocking buffer (10% fetal bovine serum in PBS, 0.05% Tween 20) at 37°C for 2 h, then washed with PBS-T (PBS + 0.05% Tween 20). The wells were then incubated with anti-FLAG M2-HRP antibody (Sigma) for 2 h at a dilution of 1:20,000 in PBS-T, and then washed with PBS-T. The peroxidase signal was detected using *o*-phenylenediamine dihydrochloride dissolved in Stable Peroxide Substrate Buffer (Pierce), followed by measurement of the absorbance signal at 450 nm using the SpectraMax 190 spectrophotometer (Molecular Devices Corporation). For normalization, and to correct for transfection efficiency, the level of GFP in each of the protein extracts was measured by fluorescence (excitation, 395 nm; emission, 507 nm) and compared with a standard of purified GFP protein (Sigma) using the Spectramax Gemini EM spectrofluorometer (Molecular Devices Corporation).

Western blot analysis was done by loading 10 μg of transfected AuxB1 cell lysates onto a 4% to 15% gradient Tris/glycine/SDS-PAGE Ready Gel (Bio-Rad). After electrophoresis, proteins were transferred to polyvinylidene difluoride membrane and probed using both anti–FLAG M2-HRP antibody and anti–GFP-HRP antibody (Santa Cruz Biotechnology), followed by detection using the enhanced chemiluminescence Western blotting system (Amersham Pharmacia).

FPGS enzyme substrate kinetics. Approximately 150 to 350 μg of total protein from AuxB1 cell lysates of FPGS allozymes was used to assay for the kinetics of either methotrexate, glutamic acid, or pemetrexed. Protein lysates were prepared via sonication in the same buffer mentioned above. Enzyme assays were done as previously described (19). For all reactions, the basic assay buffer consisted of 50 mmol/L of Tris-HCl (pH 8.5), 10 mmol/L of ATP, 10 mmol/L of KCl, 10 mmol/L of $MgCl_2$, 10 mmol/L of DTT, and 10 μmol/L of 6-diazo-5-oxo-norleucine. For antifolate kinetics, eight different concentrations of methotrexate (2–2,000 μmol/L) or a single concentration of pemetrexed (100 nmol/L) were used along with 4 mmol/L of [^{3}H]glutamic acid (10 mCi/mmol). For glutamic acid kinetics, the basic assay buffer also contained 0.25 mmol/L of methotrexate and eight different concentrations (40 μmol/L–25 mmol/L) of [^{3}H]glutamic acid (10 mCi/mmol). All reactions were done in a volume of 0.12 mL at 37°C for 1 h. Reactions were then stopped by heating at 100°C for 3 min, followed by centrifugation at 12,000 × *g* for 10 min to pellet the precipitate. The supernatant was then analyzed by high-pressure liquid chromatography (HPLC) to detect the formation of polyglutamates.

HPLC was done using a SIL-9A/SCL-6B autoinjector/controller and an LC-600 pump (Shimadzu). Fifty microliters of the sample was injected at a flow rate of 1 mL/min and separated by reverse phase HPLC on a Genesis C18 column (4.6 × 250 mm; Jones Chromatography) using a 5% to 25% acetonitrile gradient in 20 mmol/L of ammonium acetate (pH 5.0) over 20 min followed by equilibration for 10 min in 5% acetonitrile/20 mmol/L ammonium acetate (pH 5.0). Compounds were detected by a tandem configuration of UV (SPD-10AV UV-Vis Detector; Shimadzu) and radiochemical (Packard Flow Scintillation Analyzer Model 500TR; Perkin-Elmer) detectors. Methotrexate and methotrexate polyglutamates (Schircks Laboratories) were used as standards for UV detection of methotrexate polyglutamate formation, whereas pemetrexed and pemetrexed polyglutamates (Eli Lilly and Co.) were used as standards for UV detection of pemetrexed polyglutamate formation.

Folate and antifolate activity in AuxB1 cells. For analysis of methotrexate and pemetrexed dose-response, AuxB1 cells were grown in 100 mm plates in complete α(+)MEM (with 10% dialyzed fetal bovine serum), then transiently transfected with pSF-GFP FPGS allozyme expression constructs. Cells were trypsinized after 24 h, washed and resuspended in α-minimal essential medium without nucleosides [α(−)MEM, Sigma; with 10% dialyzed fetal bovine serum]. The cells were then plated at a density of 5,000 cells/well in 96-well plates in nine different concentrations of either methotrexate (1 pmol/L–100 μmol/L) or pemetrexed (0.02 nmol/L–400 μmol/L) and grown for 72 h. For analysis of folic acid dose-response, AuxB1 cells were transfected in α(+)MEM for 24 h and then transferred to 96-well plates in DMEM lacking folic acid (Sigma) and grown for 96 h in 10 different concentrations of folic acid (0.1 nmol/L–1.58 mmol/L). Cell survival/growth was analyzed using the CellTiter 96 AQueous MTS Reagent (Promega) and an electron coupling reagent, phenazine methosulfate (PMS). The 3-(4,5-dimethylthiazol-2-yl)-5(3-carboxymethonyphenol)-2-(4-sulfophenyl)-2H-tetrazolium (MTS)/PMS reagent was incubated with the cells for 2 to 4 h and the absorbance at 490 nm was measured using the SpectraMax 190 spectrophotometer (Molecular Devices Corporation). A 24-h [^{3}H]methotrexate uptake experiment was also done to determine the ratio of long-chain to short-chain polyglutamates (Supplementary Fig. S2).

FPGS complementation and generation of FPGS-AuxB1 cell lines. The ability of the FPGS allozymes to complement the *FPGS* mutation in AuxB1 cells was measured as previously described (20). DNA (10 μg) from the pSF-GFP FPGS allozyme expression constructs was used to electroporate 1×10^6 AuxB1 cells for 15 ms at 370 V. The cells were then plated at a density of 5,000 cells/plate in 60-mm plates in either α(+)MEM or α(−)MEM (with 10% dialyzed fetal bovine serum) with G418 (1.2 mg/mL; three replicates each). They were allowed to grow for 14 days and then the colonies were stained with Coomassie blue dye and counted. The percentage of colonies formed in α(−)MEM was compared with those formed in α(+)MEM. For generation of cell lines, the same electroporated AuxB1 cells were plated at a density of 250 cells/plate in 100 mm plates. After 14 days of G418 selection in α(+)MEM, colonies were picked and expanded. Expression of FPGS in different cell lines was examined by Western blot.

Data analysis and statistics. All polymorphisms observed during the resequencing were tested and found to be in Hardy-Weinberg equilibrium. Linkage disequilibrium (LD) analysis was done as described by Hartl and

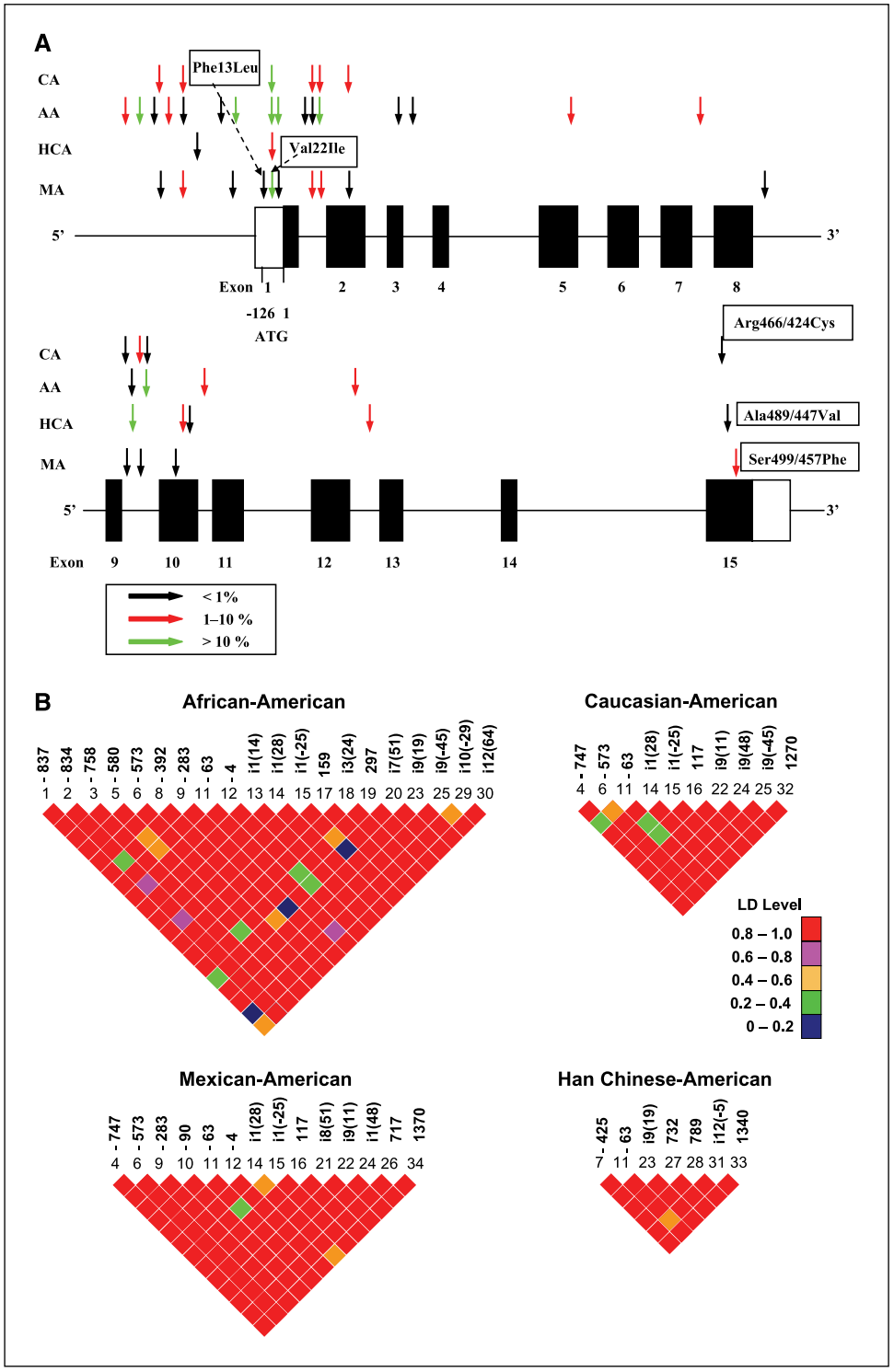

Figure 1. Human *FPGS* genetic polymorphisms. *A,* a schematic representation of the *FPGS* gene structure with the locations of polymorphisms (*arrows*). *Dark rectangles,* open reading frames; *open rectangles,* portions of exons that encode the UTR sequence. *CA,* Caucasian-American; *AA,* African-American; *HCA,* Han Chinese-American; and *MA,* Mexican-American. Changes in encoded amino acids resulting from the presence of nonsynonymous cSNPs are also indicated. SNP frequencies: *green arrows,* >10%; *red arrows,* from 1% to 10%; *black arrows,* <1%. *B,* human *FPGS* linkage disequilibrium (*LD*). Graphical depiction of the extent of population-specific LD within the area of *FPGS* resequenced, shown as pairwise *D′* values, with $P < 0.05$. The SNP number and the respective positions in the *FPGS* gene were noted.

Table 1. Human *FPGS* genetic polymorphisms

SNP no.	db−SNP identification	Location	Nucleotide	Nucleotide change	Amino acid change	Frequency of variant allele			
						African−American	Caucasian−American	Han Chinese−American	Mexican−American
1		5′−FR	−837	A → G		0.050	0.000	0.000	0.000
2		5′−FR	−834	G → T		0.317	0.000	0.000	0.000
3		5′−FR	−758	T → G		0.008	0.000	0.000	0.000
4		5′−FR	−747	C → T		0.000	0.017	0.000	0.008
5		5′−FR	−580	G → A		0.033	0.000	0.000	0.000
6		5′−FR	−573	C → G		0.008	0.067	0.000	0.017
7		5′−FR	−425	G → A		0.000	0.000	0.008	0.000
8		5′−FR	−392	G → C		0.008	0.000	0.000	0.000
9	rs10118903	5′−FR	−283	C → T		0.150	0.000	0.000	0.008
*10	rs11554717	5′−UTR(c) Exon 1(m)	−90 37	T → C	F13L	0.000	0.000	0.000	0.008
*11	rs10760502	5′−UTR(c) Exon 1(m)	−63 64	G → A	V22I	0.150	0.375	0.033	0.325
*12		5′−UTR(c) Exon 1(m)	−4 123	G → A		0.192	0.000	0.000	0.008
13		IVS 1	I1(14)	C → G		0.008	0.000	0.000	0.000
14		IVS 1	I1(28)	G → A		0.008	0.092	0.000	0.025
15	rs7586096	IVS 1	I1(−25)	A → G		0.203	0.017	0.000	0.017
16		Exon 2	117	G → A		0.000	0.017	0.000	0.008
17		Exon 3	159	G → T		0.008	0.000	0.000	0.000
18		IVS 3	I3(24)	G → C		0.008	0.000	0.000	0.000
19		Exon 5	297	C → G		0.025	0.000	0.000	0.000
20		IVS 7	I7(51)	C → T		0.093	0.000	0.000	0.000
21		IVS 8	I8(51)	A → G		0.000	0.000	0.000	0.008
22		IVS 9	I9(11)	T → C		0.000	0.008	0.000	0.008
23		IVS 9	I9(19)	G → A		0.008	0.000	0.125	0.000
24		IVS 9	I9(48)	C → T		0.000	0.042	0.000	0.008
25		IVS 9	I9(−45)	G → A		0.167	0.008	0.000	0.000
26		Exon 10	717	G → T		0.000	0.000	0.000	0.008
27		Exon 10	732	C → T		0.000	0.000	0.042	0.000
28		Exon 10	789	C → T		0.000	0.000	0.008	0.000
29		IVS 10	I10(−29)	G → A		0.075	0.000	0.000	0.000
30		IVS 12	I12(64)	A → G		0.017	0.000	0.000	0.000
31		IVS 12	I12(−5)	C → G		0.000	0.000	0.017	0.000
32		Exon 15	1270	C → T	R466/424C	0.000	0.008	0.000	0.000
33	rs17855900	Exon 15	1340	C → T	A489/447V	0.000	0.000	0.008	0.000
34		Exon 15	1370	C → T	S499/457F	0.000	0.000	0.000	0.017
					π, $\times 10^{-4}$	4.4 ± 2.7	1.9 ± 1.4	0.87 ± 0.86	1.4 ± 1.2
					u, $\times 10^{-4}$	6.8 ± 2.2	3.6 ± 1.4	2.5 ± 1.1	5.0 ± 1.7
					Tajima's D	−1.01	−1.19	−1.49	−1.91

NOTE: Polymorphism locations, alterations in nucleotide and amino acid sequences, and frequencies of polymorphisms observed are listed for each of four ethnic groups studied. Polymorphisms in exons are "boxed". Nucleotides in exons are numbered relative to the "A" in the translation initiation codon for the cytosolic (c) variant except for exon 1 which is numbered relative to the "A" in the translation initiation codon for the mitochondrial (m) variant. Asterisks refer to SNPs located in the 5′-UTR portion of the cytosolic FPGS which is also exon 1 of the mitochondrial FPGS. SNP numbers 1 to 34 are listed from the 5′-end to the 3′-end of the gene. Intron (IVS) nucleotides are numbered based on their distances from splice junctions, with the initial 5′ nucleotide in an intron designated (+1) and the final 3′ nucleotide designated (−1). The table also includes estimates of two measures of nucleotide diversity, π and u, as well as Tajima's D, a test of the "neutral" mutation hypothesis. The notation for amino acid substitution, example R466/424C, refers to the position of the substitution in the mitochondrial/cytosolic forms of FPGS, both of which are expressed by the same gene.

Clark (21) and Hendrick (22) by calculating D' values. Values for π, u, and Tajima's D were determined as described by Tajima (23). Haplotype analysis was done as described by Schaid et al. (24). The FPGS enzyme kinetic data were fitted by nonlinear regression to the Michaelis-Menten equation: $v = V_{max} \times S / (K_m + S)$, where v is the rate of reaction, V_{max} is the maximum velocity of the reaction, S is the substrate concentration, and K_m is the Michaelis constant (apparent K_m); or a modified Michaelis-Menten equation: $v = CL_{int} \times S / [1 + (S / K_m)]$, where CL_{int} is intrinsic clearance. The kinetic data was modeled using WinNonMix version 2.0.1 (Pharsight). The folic acid, methotrexate, and pemetrexed dose-response data was analyzed using GraphPad Prism version 4.0.3 (GraphPad Software). All t tests were done using GraphPad Prism version 4.0.3.

Table 2. Observed haplotype frequencies for *FPGS*

Allele	Haplotype frequency				5′−FR (−837)	5′−FR (−834)	5′−FR (−758)	5′−FR (−747)	5′−FR (−580)	5′−FR (−573)	5′−FR (−283)	5′−UTR(c)/ Exon1(m) (−63)/64	5′−UTR(c)/ Exon1(m) (−4)/123	IVS 1 I1(28)	IVS 1 I1(−25)
	AA	CA	HCA	MA											
*1A	0.330	0.427	0.816	0.609	A	G	T	C	G	C	C	G	G	G	A
*1B	0.127				A	G	T	C	G	C	T	G	A	G	G
*1C	0.108	0.348	0.025	0.291	A	G	T	C	G	C	C	A	G	G	A
*1D	0.092				A	T	T	C	G	C	C	G	G	G	A
*1E	0.067				A	T	T	C	G	C	C	G	G	G	A
*1F	0.060				A	T	T	C	G	C	C	G	G	G	A
*1G	0.042				G	T	T	C	G	C	C	G	G	G	A
*1H	0.026				A	G	T	C	A	C	C	G	A	G	G
*1I	0.018				A	G	T	C	G	C	C	G	G	G	A
*1J	0.017				A	G	T	C	G	C	C	A	G	G	A
*1K	0.015				A	T	T	C	G	C	T	G	A	G	G
*1L		0.092			A	G	T	C	G	C	C	G	G	A	A
*1M		0.048			A	G	T	C	G	G	C	G	G	G	A
*1N		0.042			A	G	T	C	G	C	C	G	G	G	A
*1O		0.010			A	G	T	C	G	G	C	A	G	G	A
*1P			0.075		A	G	T	C	G	C	C	G	G	G	A
*1Q			0.042		A	G	T	C	G	C	C	G	G	G	A
*1R				0.016	A	G	T	C	G	G	C	G	G	G	A
*2		0.008			A	G	T	T	G	C	C	A	G	G	G
*3			0.008		A	G	T	C	G	C	C	G	G	G	A
*4A				0.008	A	G	T	C	G	C	C	A	G	G	A
*4B				0.008	A	G	T	C	G	C	C	G	G	A	A

Allele	Haplotype frequency				Exon 2 117	Exon 5 297	IVS 7 I7(51)	IVS 9 I9(19)	IVS 9 I9(48)	IVS 9 I9(−45)	Exon 10 732	IVS 10 I10(−29)	Exon 15 1270	Exon 15 1340	Exon 15 1370
	AA	CA	HCA	MA											
*1A	0.330	0.427	0.816	0.609	G	C	C	G	C	G	C	G	C	C	C
*1B	0.127				G	C	C	G	C	G	C	G	C	C	C
*1C	0.108	0.348	0.025	0.291	G	C	C	G	C	G	C	G	C	C	C
*1D	0.092				G	C	T	G	C	G	C	G	C	C	C
*1E	0.067				G	C	C	G	C	G	C	A	C	C	C
*1F	0.060				G	C	C	G	C	G	C	G	C	C	C
*1G	0.042				G	C	C	G	C	G	C	G	C	C	C
*1H	0.026				G	C	C	G	C	G	C	G	C	C	C
*1I	0.018				G	G	C	G	C	G	C	G	C	C	C
*1J	0.017				G	C	C	G	C	A	C	G	C	C	C
*1K	0.015				G	C	C	G	C	G	C	G	C	C	C
*1L		0.092			G	C	C	G	C	G	C	G	C	C	C
*1M		0.048			G	C	C	G	C	G	C	G	C	C	C
*1N		0.042			G	C	C	G	T	G	C	G	C	C	C
*1O		0.010			G	C	C	G	C	G	C	G	C	C	C
*1P			0.075		G	C	C	A	C	G	C	G	C	C	C
*1Q			0.042		G	C	C	A	C	G	T	G	C	C	C
*1R				0.016	G	C	C	G	C	G	C	G	C	C	C
*2		0.008			A	C	C	G	C	G	C	G	T	C	C
*3			0.008		G	C	C	G	C	G	C	G	C	T	C
*4A				0.008	G	C	C	G	C	G	C	G	C	C	T
*4B				0.008	G	C	C	G	C	G	C	G	C	C	T

NOTE: Nucleotide positions are numbered as in Table 1. Variant nucleotides compared with the "reference sequence" (i.e., the most common sequence in African-American subjects) are highlighted as white on black. Initial haplotype designations (*1, *2, *3, and *4) were made on the basis of amino acids that vary, with the WT cytosolic sequence designated *1. Subsequent assignments/letter designations were made within ethnic groups based on decreasing frequencies.

Abbreviations: AA, African-American; CA, Caucasian-American; HCA, Han Chinese-American; MA, Mexican-American.

Results

Human *FPGS* gene resequencing. The systematic identification of genetic variation in *FPGS* was achieved through resequencing of 240 DNA samples obtained from the Coriell Cell Repository. Of these samples, 60 each were from African-American, Caucasian-American, Han Chinese American, and Mexican-American subjects. All *FPGS* exons were resequenced, including splice junctions, as well as ~1,000 bp of the 5′-flanking region of the gene.

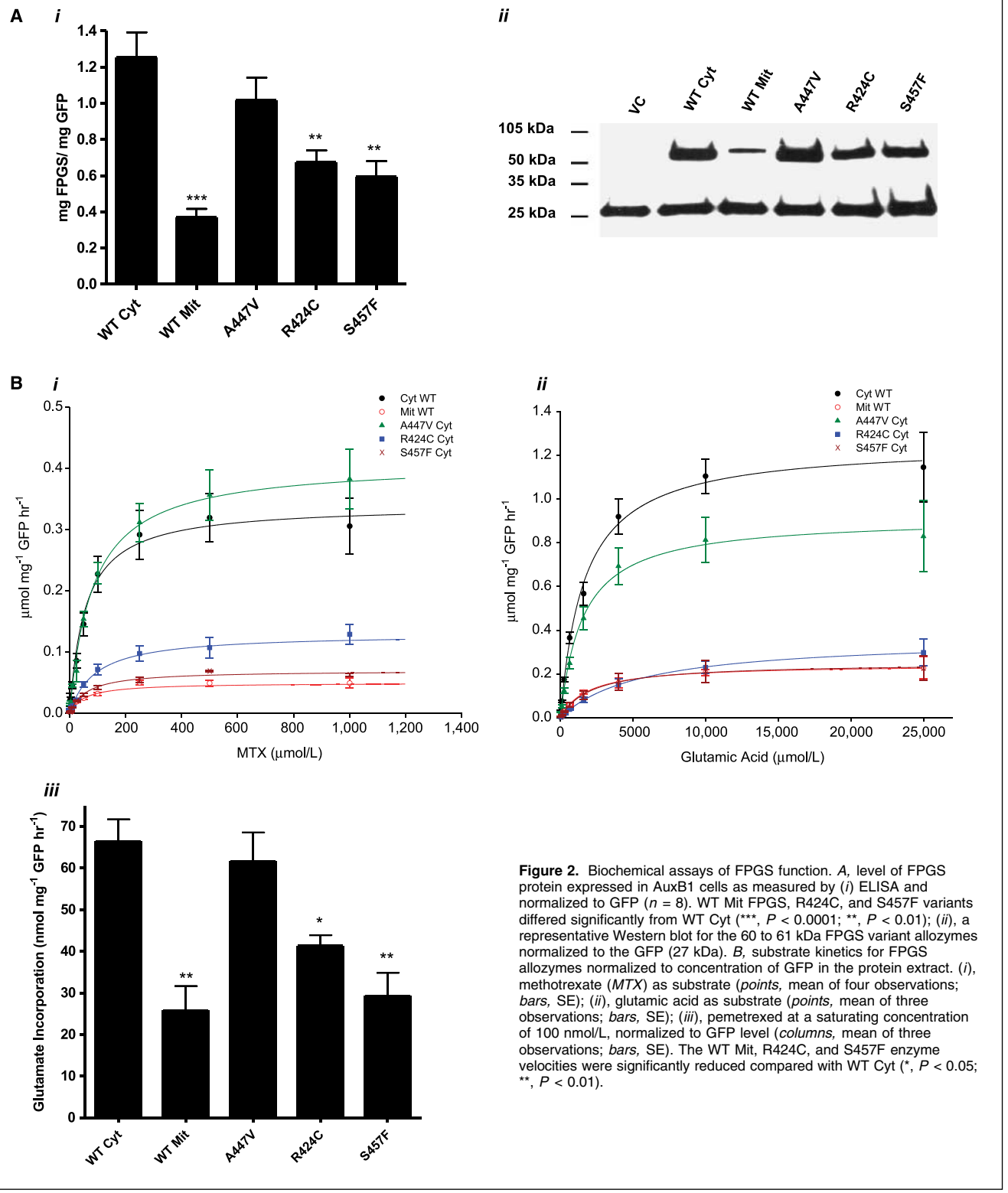

Figure 2. Biochemical assays of FPGS function. *A,* level of FPGS protein expressed in AuxB1 cells as measured by (*i*) ELISA and normalized to GFP ($n = 8$). WT Mit FPGS, R424C, and S457F variants differed significantly from WT Cyt (***, $P < 0.0001$; **, $P < 0.01$); (*ii*), a representative Western blot for the 60 to 61 kDa FPGS variant allozymes normalized to the GFP (27 kDa). *B,* substrate kinetics for FPGS allozymes normalized to concentration of GFP in the protein extract. (*i*), methotrexate (*MTX*) as substrate (*points,* mean of four observations; *bars,* SE); (*ii*), glutamic acid as substrate (*points,* mean of three observations; *bars,* SE); (*iii*), pemetrexed at a saturating concentration of 100 nmol/L, normalized to GFP level (*columns,* mean of three observations; *bars,* SE). The WT Mit, R424C, and S457F enzyme velocities were significantly reduced compared with WT Cyt (*, $P < 0.05$; **, $P < 0.01$).

Approximately 974,400 bp of the DNA sequence was analyzed as a result of resequencing these 240 DNA samples. Thirty-four polymorphisms were observed, 29 of which have not been previously reported (Fig. 1*A*; Table 1). Twenty-one of the SNPs were "common", with allele frequencies of >1% in at least one ethnic group and one SNP was common to all four populations. There were large differences among these ethnic groups both in allele frequency and type, with 20 polymorphisms in African-American DNA, 10 in DNA samples from Caucasian-American subjects, 7 in Han Chinese-American subjects, and 14 in DNA from Mexican-American subjects. Twelve specific polymorphisms were observed only in the African-American population, one in Caucasian-American subjects, five in Han Chinese-American subjects, and four in Mexican-American subjects. We also determined "nucleotide diversity," a quantitative measure of genetic variation, adjusted for the number of alleles studied. Two standard measures of nucleotide diversity are π, average heterozygosity per site, and u, a population measure that is theoretically equal to the neutral mutation variable (25). These values are listed in Table 1, with the African-American subjects showing greater nucleotide diversity than the other groups. In addition, values for Tajima's *D*, a test of the "neutral" mutation hypothesis (23), were estimated for each population (Table 1). Under conditions of neutrality, Tajima's *D* should equal 0. The negative values for Tajima's *D* (Table 1), suggest a departure from neutrality; however, the *P* values were >0.05 and therefore not significant, except for the Mexican-American group ($P = 0.051$), which is suggestive of a trend towards departure from the neutral hypothesis.

Five nonsynonymous cSNPs, polymorphisms that altered the encoded amino acids, were observed: F13L and V22I, which are present only in the mitochondrial form of FPGS, and R466/424C, A489/447V, and S499/457F, which are present in both mitochondrial and cytosolic forms of FPGS (Fig. 1*A*; Table 1). The SNPs resulting in F13L, V22I, and A489/447V have previously been observed (26) but no functional data has been published. The V22I polymorphism was very common, and was present in all of the populations with allele frequencies of 15% in African-American samples, 37.5% in Caucasian-American samples, 3.3% in Han Chinese-American samples, and 32.5% in Mexican-American samples. The F13L and S499/457F polymorphisms were only observed in the Mexican-American population, with allele frequencies of 0.8% and 1.7%, respectively. The R466/424C polymorphism was present only in the Caucasian-American subjects with an allele frequency of 0.8%, whereas the A489/447V polymorphism was present only in the Han Chinese-American subjects with an allele frequency of 0.8%.

LD and haplotype analysis. Haplotype information may be more useful than individual polymorphisms for application in association studies (27, 28). We therefore did population-specific LD and haplotype analyses for the 34 SNPs that we observed in *FPGS*. For the LD analysis, D' values were calculated for all pairwise combinations of SNPs. D' values can range from 1.0, when two polymorphisms are maximally associated, to 0 when they are randomly associated (21, 22). A graphical representation of the LD is depicted in Fig. 1*B* for D' values with $P \leq 0.05$. Haplotypes can be determined unequivocally only if no more than one polymorphism in an allele is heterozygous, but it is also possible to infer haplotypes computationally (24). Twenty-two unequivocal haplotypes were identified with a great deal of variation among the four ethnic groups studied (Table 2). The inferred haplotypes are available upon request. Five haplotypes included the V22I polymorphism, the polymorphism that was common to all four populations. The major haplotype containing this polymorphism, designated as **1C*, was the most common in Caucasian-American subjects at 34.8%. The **1C* haplotype was present at a frequency of 10.8% in African-American subjects, 2.5% in Han Chinese-American subjects, and 29.1% in Mexican-American subjects. The S499/457F polymorphism was found in two separate haplotypes (**4A* and **4B*), both in the Mexican-American samples, with a frequency of 0.8%. The other polymorphisms, R466/424C (**2* haplotype) and A489/447V (**3* haplotype), occurred at a frequency of 0.8% in both Caucasian-American and Han Chinese-American subjects.

Recombinant allozyme protein expression. The functional significance of the three cytosolic *FPGS* nonsynonymous cSNPs that were discovered from gene resequencing was studied by expressing the cDNAs in AuxB1 cells. AuxB1 cells are an ideal system in which to study FPGS activity because they lack endogenous enzyme activity and must be supplemented with a source of nucleotides in the growth medium to compensate for this deficiency (29). The cDNAs for the FPGS allozymes were cloned into a vector with a bi-cistronic expression cassette so that expression was upstream of GFP on the same mRNA. This allows for normalization of differences in transfection efficiency and mRNA stability. An NH_2-terminal FLAG epitope was attached to allow for the detection and quantification of the immunoreactive protein. We focused on analyzing the variant cytosolic allozymes because previous studies had shown that methotrexate and its polyglutamate derivatives were not detected in the mitochondria (30). The concentration of WT Cyt FPGS protein was ~1.25 mg/mg of GFP as measured by ELISA (Fig. 2*A, i*), 3.4-fold higher than the mitochondrial form of the protein. Expression of the A447V variant was comparable to the WT Cyt form, whereas the R424C and S457F variants were reduced by 1.86- and 2.11-fold, respectively. This pattern of protein expression can be seen in the relative intensity of the 60- to 61-kDa bands of the Western blot in Fig. 2*A* (*ii*).

Recombinant allozyme kinetics. To determine whether *FPGS* polymorphisms affect the ability of the allozymes to catalyze the addition of glutamate to pteroyl-glutamate, the *in vitro* activity of the variants was measured with different substrates. The Michaelis-Menten kinetic plots for methotrexate and glutamic acid are shown in Fig. 2*B* (*i* and *ii*). Methotrexate diglutamate was detected as the only product in both assays. The methotrexate Michaelis-Menten plots for the WT Cyt and the A447V allozymes seem to be quite similar, whereas the R424C and S457F variants have reduced activity (Fig. 2*B, i*). The K_m of methotrexate for the variant allozymes was not significantly different from that of the WT Cyt enzyme, whereas the apparent methotrexate V_{max} for both the R424C and S457F variants were significantly reduced (Table 3). More importantly, the intrinsic clearance (V_{max}/K_m) of methotrexate was significantly reduced compared with WT Cyt for both the R424C (4.2-fold) and S457F (5.4-fold) allozymes (Table 3). The difference between the allozymes is more dramatic when one examines the substrate kinetics of glutamic acid (Fig. 2*B, ii*). The K_m of glutamic acid in the R424C variant was increased 3.5-fold, whereas the apparent V_{max} was reduced 3.4-fold (Table 3), which resulted in a 12.3-fold decrease in intrinsic clearance of glutamic acid. The glutamic acid K_m in the S457F variant was not significantly altered compared with WT Cyt, but the apparent V_{max} was reduced 5-fold, which resulted in a 6.2-fold drop in intrinsic clearance of glutamic acid.

The R424C and S457F polymorphisms also influenced the enzyme activity with pemetrexed as a substrate (Fig. 2*B, iii*). The velocities of the WT Mit, R424C, and S457F allozymes at 100 nmol/L of pemetrexed were significantly reduced compared with the WT Cyt form (Fig. 2*B, iii*). Only saturating concentrations of pemetrexed (100 nmol/L) were used for this experiment because it was found that at low pemetrexed concentrations, the enzyme did not exhibit steady state kinetics due to the formation of high-affinity polyglutamates (data not shown).

Effect of polymorphisms on folate and antifolate activity in culture. Based on the *in vitro* kinetics of the allozymes, it was suspected that the presence of the R424C and S457F polymorphisms in *FPGS* may affect the metabolism and activity of folates and antifolates in cell culture. AuxB1 cells transfected with the variant *FPGS* cDNAs were grown in the presence of different concentrations of folic acid, methotrexate, or pemetrexed and cell growth/survival was measured by MTS assay (Fig. 3). The folic acid dose-response curve for the A447V allozyme was very similar to that of the WT Cyt form, whereas the curves for the WT Mit, R424C, and S457F variants were shifted to the right (Fig. 3*A*). This corresponds to an increase in the EC_{50} for folic acid of 4.28-fold for the WT Mit protein, 4.32-fold for the R424C variant, and 4.28-fold for the S457F variant (Table 3). The clonogenic survival of AuxB1 cells expressing these two polymorphisms was also reduced when grown in 2.2 μmol/L of folic acid [α(−)MEM without nucleosides] compared with WT Cyt (Fig. 3*B*). Additionally, the activity of methotrexate was reduced in AuxB1 cells expressing the R424C and S457F allozymes, although the effect was not as dramatic as that seen for folic acid (Fig. 3*C*). The IC_{50} of methotrexate in cells expressing the R424C variant was 1.84-fold higher than in cells expressing WT Cyt FPGS, 1.64-fold higher in cells expressing the S457F variants, and 1.52-fold higher in cells expressing the WT Mit variant (Table 3). Cells expressing the A447V allozyme also displayed a slightly higher IC_{50} for methotrexate than for WT Cyt, but this difference was not significant. The reduced efficacy of methotrexate in the R424C and S457F variants is confirmed by measuring the formation of long-chain polyglutamates during 24 h uptake of [^{3}H]methotrexate (Supplementary Fig. S2). These experiments showed that these two variants accumulate a lower ratio of long-chain methotrexate polyglutamates (MTX-G7, MTX-G8, and MTX-G9) to short-chain polyglutamates (MTX-G4, MTX-G5, and MTX-G6) when compared with WT Cyt or A447V (Supplementary Fig. S2). The di- and triglutamates of methotrexate were not detected intracellularly after the 24-h incubation.

The dose-response curve for pemetrexed is shown in Fig. 3*D* and the results were similar to those seen with methotrexate. The greatest increase in the IC_{50} of pemetrexed was seen in cells expressing the cytosolic S457F allozyme, which showed a 2.2-fold increase compared with cells expressing the WT Cyt enzyme (Table 3). The R424C cytosolic variant displayed an increase in IC_{50} of 1.9-fold with respect to the WT Cyt variant (Table 3).

Discussion

The folate pathway is an important target for anticancer therapeutics, and FPGS is one of its key enzymes. Many folates and antifolates are metabolized to their polyglutamate form by this enzyme. Because polyglutamation results in dramatic increases in affinity for target enzymes, it is important to identify genetic variation in *FPGS* and determine its effect on the response of cancer patients to both antifolate therapy and folate supplementation. In this study, we have taken a systematic approach to identify polymorphisms in *FPGS* and then characterize their effect on the function of this enzyme. We observed 29 polymorphisms that have not been previously identified. Two of the five nonsynonymous cSNPs that were identified, R466/424C and S499/457F, are novel. The R424C polymorphism, when expressed in the cytosolic form of the protein, caused a reduction in the intrinsic clearance of glutamic acid and methotrexate, and an increase in the K_m for glutamate compared with WT Cyt. The S457F polymorphism also caused a reduction in the intrinsic clearance for both glutamic acid and methotrexate; however, the K_m for both substrates was not different from the WT Cyt values.

Table 3. Functional variables of FPGS allozymes

Variable	WT Cyt	WT Mit	A447V	R424C	S457F
MTX, V_{max} (μmol mg^{-1} GFP h^{-1})	0.34 ± 0.06	0.05 ± 0.01*	0.41 ± 0.08	0.13 ± 0.03†	0.07 ± 0.002*
MTX, K_m (μmol/L)	55.5 ± 6.06	52.6 ± 11.7	82.7 ± 16.0	90.8 ± 20.5	61.3 ± 4.40
MTX, V_{max}/K_m (mL mg^{-1} GFP h^{-1})	6.03 ± 1.05	1.02 ± 0.13*	4.90 ± 2.88	1.44 ± 0.18*	1.12 ± 0.09*
GA, V_{max} (μmol mg^{-1} GFP h^{-1})	1.26 ± 0.14	0.25 ± 0.04*	0.92 ± 0.15	0.37 ± 0.07*	0.25 ± 0.06*
GA, K_m (μmol/L)	1702 ± 255	2068 ± 351	1630 ± 213	5984 ± 532*	2281 ± 300
GA, V_{max}/K_m (mL mg^{-1} GFP h^{-1})	0.74 ± 0.13	0.13 ± 0.03†	0.59 ± 0.14	0.06 ± 0.01*	0.12 ± 0.04†
FA, EC_{50} (nmol/L)	357.0 ± 97.9	1530.0 ± 274†	348.0 ± 63.6	1540.0 ± 371†	1530.0 ± 226*
MTX, IC_{50} (nmol/L)	9.5 ± 1.08	14.5 ± 2.44†	12.9 ± 1.68	17.5 ± 2.09*	15.6 ± 2.19†
PMX, IC_{50} (nmol/L)	13.6 ± 1.27	11.0 ± 1.61	12.7 ± 1.42	26.3 ± 3.69*	30.2 ± 2.95‡

NOTE: Apparent V_{max} and V_{max}/K_m (intrinsic clearance) values are shown for glutamic acid and methotrexate. Values indicate mean ± SE for three and four experiments, respectively, and normalized to GFP protein level. The EC_{50} and IC_{50} values represent the mean ± SE for folic acid (three experiments), methotrexate (five experiments), and pemetrexed (six observations). Variant allozymes differed significantly from WT Cyt allozyme.
Abbreviations: GA, glutamic acid; MTX, methotrexate; FA, folic acid; PMX, pemetrexed.
*$P < 0.01$.
†$P < 0.05$.
‡$P < 0.001$ (independent t test).

Both polymorphisms increased the EC_{50} values for folic acid and the IC_{50} values for methotrexate and pemetrexed in AuxB1 cells expressing these cytosolic allozymes. The increased IC_{50} for methotrexate is probably due to a reduction in the relative proportion of high-affinity long-chain methotrexate polyglutamates versus lower affinity short-chain methotrexate polyglutamates in the R424C and S457F variants when compared with the WT Cyt variant (Supplementary Fig. S2). This same mechanism may also be responsible for the increase in IC_{50} in these two variants when compared with WT Cyt that was observed with pemetrexed.

The crystal structure of human FPGS has not been solved, however, the structures of the *Escherichia coli, Lactobacillus casei*, and *Mycobacterium tuberculosis* proteins have been published (31–34). Human FPGS has been successfully modeled to the structure of the *L. casei* protein using homology modeling algorithms (17). Therefore, to understand why alteration of R424C and S457F may cause these changes in FPGS kinetics, whereas the A447V substitution does not, we examined the SNP positions in the three-dimensional structure of human FPGS. This structure was generated by homology modeling to the published *L. casei*

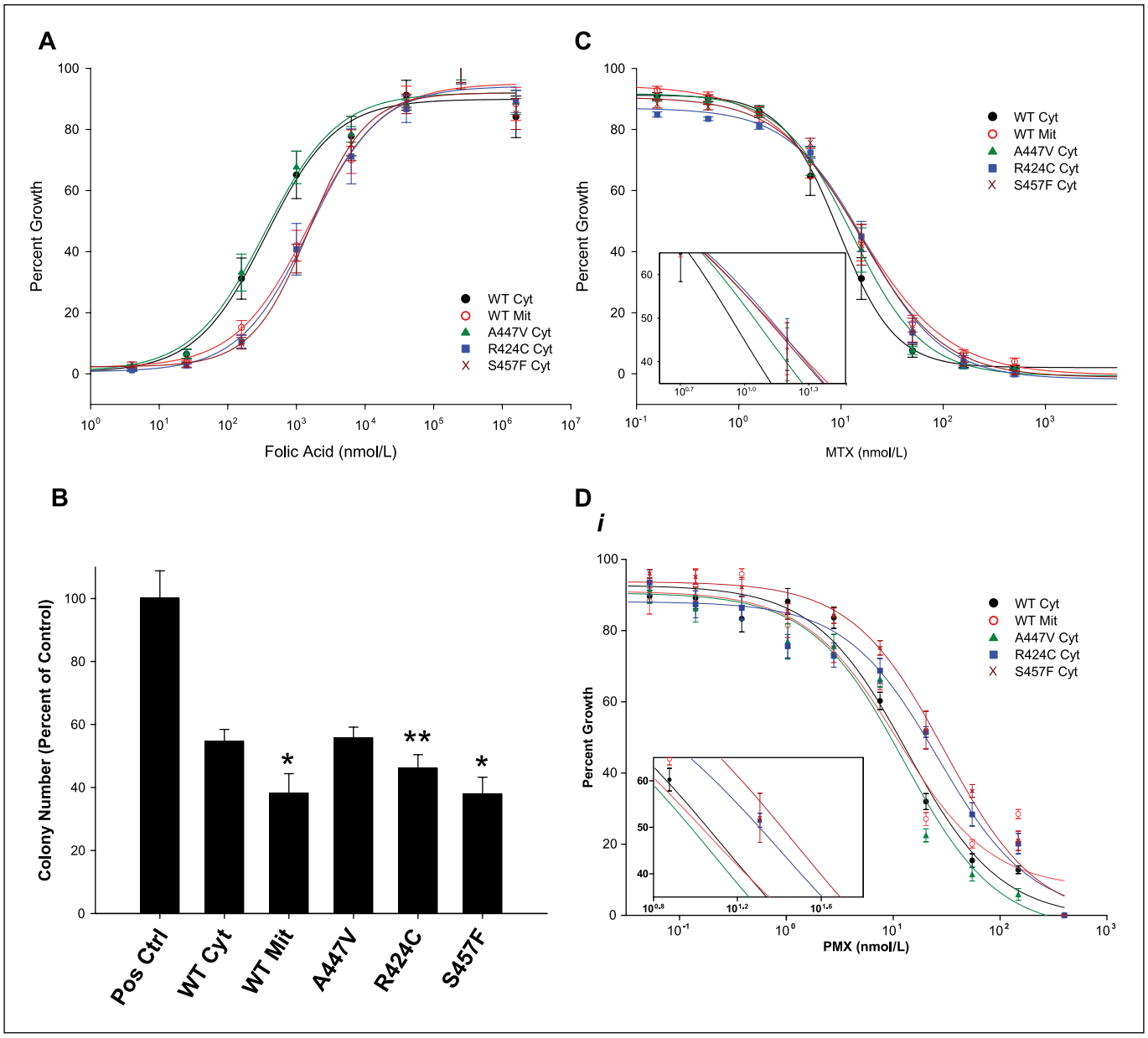

Figure 3. Activity of folic acid, methotrexate, and pemetrexed in cells expressing FPGS allozymes. *A*, dose-response curve for folic acid (*points,* mean of three observations; *bars,* SE). *B*, clonogenic growth of AuxB1 cells transfected with FPGS variant cDNAs, and grown in $\alpha(-)$MEM containing 2.2 μmol/L of folic acid. Cells transfected with WT Mit FPGS and the R424C and S457F variants produced 30%, 15%, and 30% fewer colonies, respectively, than those transfected with WT Cyt FPGS (*, $P < 0.05$, **, $P < 0.01$). Colony numbers are expressed as a percentage of colonies formed (*columns,* mean; *bars,* SE) compared with each variant grown in $\alpha(+)$MEM. *C,* dose-response curve for methotrexate (*points,* mean of five observations; *bars,* SE). *Inset,* an expanded portion of the dose-response curve surrounding the IC_{50}. *D,* dose-response curve for pemetrexed (*points,* mean of six observations; *bars,* SE). *Inset,* an expanded portion of the dose-response curve surrounding the IC_{50}.

protein structure using the Swiss-Model resource (ref. 35; Supplementary Fig. S1). All three amino acids are positioned in the COOH-terminal domain of the protein, outside of the binding sites for glutamic acid, pteroyl-glutamate, and ATP (34). Mutations near these substrate binding sites have been shown to abolish FPGS activity (36, 37). Because neither R424, A447, nor S457 are in the vicinity of these substrate-binding sites, it is unlikely that these amino acid alterations would abolish enzyme activity. Amino acid substitutions in the C domain have been shown to reduce FPGS activity by varying degrees (16, 17), so it is possible that the R424C and S457F substitutions, which are chemically dramatic alterations, could influence the three-dimensional structure of FPGS enough to disrupt folate and/or glutamic acid binding, a change that was observed when their substrate kinetics were compared with the WT Cyt enzyme (Fig. 2*B*; Table 3). Conversely, the A447V substitution is unlikely to affect enzyme activity given the fact that it is a chemically conservative substitution, resulting in properties that are similar to the WT Cyt enzyme (Fig. 2*B*; Table 3).

The C424 and F457 polymorphisms not only caused disruption of FPGS enzyme kinetics, but also caused a reduction in protein expression (Fig. 2*A*). The mechanism for this reduction is probably due to increased protein degradation or increased aggregation resulting from protein misfolding as has been implicated in numerous pharmacogenomic studies of SNPs (38–41). It is likely that the combination of reduced protein level and altered enzyme kinetics contribute to the increase in EC_{50} for folic acid and IC_{50} for both methotrexate and pemetrexed seen in AuxB1 cells expressing the Cys424 and Phe457 allozymes (Table 3).

The reduced efficacy of pemetrexed, methotrexate, and folic acid in cells expressing the R424C and S457F polymorphisms of *FPGS* are suggestive of pharmacogenomic implications in patients undergoing antifolate therapy. Patients with these genotypes may need higher doses of drug to reach the same level of intracellular polyglutamates as patients who have the WT genotype. Additionally, they may require higher doses of folic acid or leucovorin to reduce cytopenia. The R424C and S457F polymorphisms may also cause a reduction in the accumulation of long-chain antifolate polyglutamates, which may correlate with reduced efficacy in patients with these genotypes. In summary, we have systematically applied a genotype-to-phenotype strategy to study *FPGS*, a gene in the folate pathway that plays a critical role as an important target for anticancer therapeutics. The genomics and functional characterization will make it possible to correlate individual genetic variations with risk for toxicity and response to antifolate therapy and efficacy.

Acknowledgments

Received 1/15/2007; revised 6/20/2007; accepted 7/5/2007.

The costs of publication of this article were defrayed in part by the payment of page charges. This article must therefore be hereby marked *advertisement* in accordance with 18 U.S.C. Section 1734 solely to indicate this fact.

The authors thank Dr. Richard Weinshilboum for his ongoing advice during this project and for making it possible to perform the resequencing studies in his laboratory.

References

1. Jolivet J, Cowan KH, Curt GA, Clendeninn NJ, Chabner BA. The pharmacology and clinical use of methotrexate. N Engl J Med 1983;309:1094–104.
2. Adjei AA. Pemetrexed (ALIMTA), a novel multitargeted antineoplastic agent. Clin Cancer Res 2004;10:4276–80s.
3. Mendelsohn LG, Shih C, Chen VJ, Habeck LL, Gates SB, Shackelford KA. Enzyme inhibition, polyglutamation, and the effect of LY231514 (MTA) on purine biosynthesis. Semin Oncol 1999;26:42–7.
4. Kumar P, Kisliuk RL, Gaumont Y, Freisheim JH, Nair MG. Inhibition of human dihydrofolate reductase by antifolyl polyglutamates. Biochem Pharmacol 1989;38:541–3.
5. Zhao R, Goldman ID. Resistance to antifolates. Oncogene 2003;22:7431–57.
6. Moran RG, Werkheiser WC, Zakrzewski SF. Folate metabolism in mammalian cells in culture. I. Partial characterization of the folate derivatives present in L1210 mouse leukemia cells. J Biol Chem 1976;251:3569–75.
7. Schirch V, Strong WB. Interaction of folylpolyglutamates with enzymes in one-carbon metabolism. Arch Biochem Biophys 1989;269:371–80.
8. Shih C, Habeck LL, Mendelsohn LG, Chen VJ, Schultz RM. Multiple folate enzyme inhibition: mechanism of a novel pyrrolopyrimidine-based antifolate LY231514 (MTA). Adv Enzyme Regul 1998;38:135–52.
9. Whitehead VM, Rosenblatt DS, Vuchich MJ, Shuster JJ, Witte A, Beaulieu D. Accumulation of methotrexate and methotrexate polyglutamates in lymphoblasts at diagnosis of childhood acute lymphoblastic leukemia: a pilot prognostic factor analysis. Blood 1990;76:44–9.
10. Masson E, Relling MV, Synold TW, et al. Accumulation of methotrexate polyglutamates in lymphoblasts is a determinant of antileukemic effects *in vivo*. A rationale for high-dose methotrexate. J Clin Invest 1996;97:73–80.
11. UCSC Genome Browser. 2006. Available from: http://www.genome.ucsc.edu/cgi-bin/htGateway.
12. Taylor SM, Freemantle SJ, Moran RG. Structural organization of the human folypoly-γ-glutamate synthetase gene: evidence for a single genomic locus. Cancer Res 1995;55:6030–4.
13. Freemantle SJ, Taylor SM, Krystal G, Moran RG. Upstream organization of and multiple transcripts from the human folylpoly-γ-glutamate synthetase gene. J Biol Chem 1995;270:9579–84.
14. Wang Y, Zhao R, Goldman ID. Decreased expression of the reduced folate carrier and folypolyglutamate synthetase is the basis for acquired resistance to the pemetrexed antifolate (LY231514) in an L1210 murine leukemia cell line. Biochem Pharmacol 2003;65:1163–70.
15. El-Fadili A, Richard D, Kundig C, Ouellette M. Effect of polyglutamylation of methotrexate on its accumulation and the development of resistance in the protozoan parasite Leishmania. Biochem Pharmacol 2003;66:999–1008.
16. Zhao R, Titus S, Gao F, Moran RG, Goldman ID. Molecular analysis of murine leukemia cell lines resistant to 5,10-dideazatetrahydrofolate identifies several amino acids critical to the function of folylpolyglutamate synthetase. J Biol Chem 2000;275:26599–606.
17. Liani E, Rothem L, Bunni MA, Smith CA, Jansen G, Assaraf YG. Loss of folylpoly-γ-glutamate synthetase activity is a dominant mechanism of resistance to polyglutamylation-dependent novel antifolates in multiple human leukemia sublines. Int J Cancer 2003;103:587–99.
18. Ma CX, Adjei AA, Salavaggione OE, et al. Human aromatase: gene resequencing and functional genomics. Cancer Res 2005;65:11071–82.
19. Sanghani PC, Moran RG. Purification and characteristics of recombinant human folylpoly-γ-glutamate synthetase expressed at high levels in insect cells. Protein Expr Purif 2000;18:36–45.
20. Turner FB, Taylor SM, Moran RG. Expression patterns of the multiple transcripts from the folylpolyglutamate synthetase gene in human leukemias and normal differentiated tissues. J Biol Chem 2000;275:35960–8.
21. Hartl DL, Clark AG. Organization of genetic variation. In: Principles of population genetics, Chapter 3. 3rd ed. Sunderland (MA): Sinauer Associates, Inc; 2000. p. 95–107.
22. Hendrick PW. Genetics of populations. 3rd ed. Sundbury (MA): Jones and Bartlett Publishers; 2000.
23. Tajima F. Statistical method for testing the neutral mutation hypothesis by DNA polymorphism. Genetics 1989;123:585–95.
24. Schaid DJ, Rowland CM, Tines DE, Jacobson RM, Poland GA. Score tests for association between traits and haplotypes when linkage phase is ambiguous. Am J Hum Genet 2002;70:425–34.
25. Fullerton SM, Clark AG, Weiss KM, et al. Apolipoprotein E variation at the sequence haplotype level: implications for the origin and maintenance of a major human polymorphism. Am J Hum Genet 2000;67:881–900.
26. Sherry ST, Ward M, Sirotkin K. dbSNP-database for single nucleotide polymorphisms and other classes of minor genetic variation. Genome Res 1999;9:677–9.
27. Brodde OE, Leineweber K. β2-Adrenoceptor gene polymorphisms. Pharmacogenet Genomics 2005;15:267–75.
28. Drysdale CM, McGraw DW, Stack CB, et al. Complex promoter and coding region β2-adrenergic receptor haplotypes alter receptor expression and predict *in vivo* responsiveness. Proc Natl Acad Sci U S A 2000;97:10483–8.
29. Taylor RT, Wu R, Hanna ML. Induced reversion of a Chinese hamster ovary triple auxotroph. Validation of the system with several mutagens. Mutat Res 1985;151:293–308.
30. Qi H, Atkinson I, Xiao S, Choi YJ, Tobimatsu T, Shane B. Folylpoly-γ-glutamate synthetase: generation of isozymes and the role in one carbon metabolism and antifolate cytotoxicity. Adv Enzyme Regul 1999;39:263–73.

31. Sun X, Bognar AL, Baker EN, Smith CA. Structural homologies with ATP- and folate-binding enzymes in the crystal structure of folylpolyglutamate synthetase. Proc Natl Acad Sci U S A 1998;95:6647–52.
32. Mathieu M, Debousker G, Vincent S, Viviani F, Bamas-Jacques N, Mikol V. *Escherichia coli* FolC structure reveals an unexpected dihydrofolate binding site providing an attractive target for anti-microbial therapy. J Biol Chem 2005;280:18916–22.
33. Young PG, Smith CA, Sun X, Baker EN, Metcalf P. Purification, crystallization and preliminary X-ray analysis of *Mycobacterium tuberculosis* folylpolyglutamate synthase (MtbFPGS). Acta Crystallograph Sect F Struct Biol Cryst Commun 2006;62:579–82.
34. Sun X, Cross JA, Bognar AL, Baker EN, Smith CA. Folate-binding triggers the activation of folylpolyglutamate synthetase. J Mol Biol 2001;310:1067–78.
35. Schwede T, Kopp J, Guex N, Peitsch MC. SWISS-MODEL: an automated protein homology-modeling server. 2003 [cited 2006; Available from: http://swissmodel.expasy.org/.
36. Smith CA, Cross JA, Bognar AL, Sun X. Mutation of Gly51 to serine in the P-loop of *Lactobacillus casei* folylpolyglutamate synthetase abolishes activity by altering the conformation of two adjacent loops. Acta Crystallogr D Biol Crystallogr 2006;62:548–58.
37. Sheng Y, Cross JA, Shen Y, Smith CA, Bognar AL. Mutation of an essential glutamate residue in folylpolyglutamate synthetase and activation of the enzyme by pteroate binding. Arch Biochem Biophys 2002;402:94–103.
38. Wang L, Yee VC, Weinshilboum RM. Aggresome formation and pharmacogenetics: sulfotransferase 1A3 as a model system. Biochem Biophys Res Commun 2004;325:426–33.
39. Ji Y, Salavaggione OE, Wang L, et al. Human phenylethanolamine N-methyltransferase pharmacogenomics: gene re-sequencing and functional genomics. J Neurochem 2005;95:1766–76.
40. Mukherjee B, Salavaggione OE, Pelleymounter LL, et al. Glutathione S-transferase ω1 and ω2 pharmacogenomics. Drug Metab Dispos 2006;34:1237–46.
41. Wang L, Sullivan W, Toft D, Weinshilboum R. Thiopurine S-methyltransferase pharmacogenetics: chaperone protein association and allozyme degradation. Pharmacogenetics 2003;13:555–64.